NÖHÜ Müh. Bilim. Derg. / NOHU J. Eng. Sci., 2024; 13(3), 882-891

Niğde Ömer Halisdemir Üniversitesi Mühendislik Bilimleri Dergisi
Niğde Ömer Halisdemir University Journal of Engineering Sciences

Araştırma makalesi / Research article

www.dergipark.org.tr/tr/pub/ngumuh / www.dergipark.org.tr/en/pub/ngumuh

Drought monitoring in Burdur Lake using Sentinel-2 images

Sentinel-2 görüntüleri kullanılarak Burdur Gölü'nde kuraklık izleme

Ümit Haluk Atasever [1], Hussein Hadi Abbas [2,*]

[1,2] *Erciyes University, Engineering faculty, Department of Map Engineering. Kayseri, Türkiye.*
[2] *Ministry of Transport, Contracts and Licensing Office, Baghdad, Iraq.*

Abstract

This study presents an automated workflow for drought monitoring in Burdur Lake, Turkey, utilizing Sentinel-2 satellite data and K-means clustering. Five Sentinel-2 images from 2019 to 2023 were processed to derive spectral water indices. A water mask was generated by thresholding the indices, allowing for the distinction of water bodies. K-means clustering quantified changes in the lake area over time. The results reveal a decreasing trend in water extent from August 2019 to August 2023. In August 2019, the water extent was approximately 18.53% (138.9456 Km2), which declined to around 16.64% (124.7500 Km^2) by August 2023, signifying an approximately 10.3% reduction in water extent between the start and end years. This approach demonstrates a valuable framework for the integration of freely available satellite data and machine learning algorithms in operational drought monitoring.

Keywords: Drought monitoring, Water mask, Sentinel-2 imagery, K-Means clustering, Burdur Lake Türkiye

Özet

Bu çalışma, Burdur Gölü'nde kuraklık izlemesi için Sentinel-2 uydu verileri ve K-means kümeleme kullanılarak otomatik bir iş akışı sunmaktadır. 2019'dan 2023'e kadar beş Sentinel-2 görüntüsü, spektral su indekslerini üretmek için işlenmiştir. Su indekslerinin eşiklenmesiyle bir su maskesi oluşturulmuş, böylece su kütlelerinin ayırt edilmesi sağlanmıştır. K-means kümeleme, zaman içinde göl alanındaki değişiklikleri ölçümlenmiştir. Sonuçlar, Ağustos 2019'dan Ağustos 2023'e kadar su genişliğinde azalan bir eğilim ortaya koymaktadır. Ağustos 2019'da su genişliği yaklaşık %18.53 (138.9456 Km^2) iken, Ağustos 2023'e kadar yaklaşık %16.64'e (124.7500 Km^2) düşmüş, başlangıç ve bitiş yılları arasında yaklaşık %10.3'lük bir su genişliği azalmasına işaret etmektedir. Bu yaklaşım, serbestçe erişilebilir uydu verileri ve makine öğrenmesi algoritmalarının operasyonel kuraklık izlemeye entegrasyonu için değerli bir çerçeve sunmaktadır.

Anahtar kelimeler: Kuraklık izleme, Su maskesi, Sentinel-2 görüntüleme, K-Means kümeleme, Burdur Gölü Türkiye

1 Introduction

Effective water resources management, especially in regions under continuous climate variability as well as anthropogenic pressures, demands detailed monitoring and mapping of variations in lake water bodies. Temporal fluctuations in the lake areas are studied effectively using time series analysis of satellite images through remote sensing technologies [1], [2].The dynamic and heterogeneous nature of lake shorelines poses challenges for accurate mapping, necessitating automated algorithms for operational monitoring of lake extent changes [3], [4].

Burdur Lake, nestled in the scenic landscapes of Turkey, has played a crucial role in the ecological and socio-economic fabric of the region. Characterized by its semi-arid climate, Burdur Lake has faced significant declines in water level and area in recent decades, primarily due to climatic factors and human activities [5]. The lake, spanning approximately 250 square kilometers, has been a subject of concern and study, given its vulnerability to changing environmental conditions [5].

Early studies on Burdur Lake primarily relied on optical satellite imagery but often encountered limitations, such as the need for manual digitization of lake boundaries [5]. The complexity of the lake's shoreline, coupled with the challenges posed by climate and human-induced changes, necessitates more advanced and automated methodologies for comprehensive monitoring.

Spectral water indices such as NDWI and MNDWI have proven to be effective in enhancing the identification of open water areas across different landscapes like lakes. [6], [7]. These indices leverage the unique spectral signatures of water bodies, enabling precise discrimination between water and non-water pixels. Furthermore, the application of thresholding techniques on these indices results in binary water masks, facilitating the classification of pixels into distinct categories of water and non-water [7], [8].

Machine learning clustering algorithms, particularly K-means clustering, have shown potential in categorizing land cover types based on spectral characteristics [9], [10]. This study aims to build upon the foundation laid by previous research on Burdur Lake, introducing a comprehensive methodology for drought monitoring. By integrating Sentinel-2 image time series and leveraging advanced spectral indices, including NDWI, MNDWI, and AWEI, this study seeks to quantify changes in Burdur Lake's water extent over the years 2019 to 2023.

The significance of this automated workflow lies not only in its capacity to provide timely and accurate insights into Burdur Lake's drought conditions but also in its potential

* Sorumlu yazar / Corresponding author, e-posta / e-mail: eng.hussein96@yahoo.com (H. H. Abbas)
Geliş / Recieved: 29.12.2023 Kabul / Accepted: 15.05.2024 Yayımlanma / Published: 15.07.2024
doi: 10.28948/ngumuh.1411803

applicability to other regional water bodies. By harnessing the readily available Sentinel-2 data, this approach contributes to proactive water management efforts, crucial in the face of evolving climate patterns and human activities.

2 Material and methods

2.1 Study area and satellite data

Burdur Lake (Northwest Corner: Latitude 37.857, Longitude 30.034, Southeast Corner: Latitude 37.619, Longitude 30.353) is in a closed basin in southwestern Turkey as seen in Figure 1.

Figure 1. Burdur Lake

Five Sentinel-2 L1C images were acquired during August from 2019 to 2023 which are:

- S2B_MSIL2A_20190830T083609_N0213_R064_T35SQB_20190830T123940.SAFE
- S2B_MSIL2A_20200827T084559_N0214_R107_T35SQB_20200827T113630.SAFE
- S2B_MSIL2A_20210829T083559_N0500_R064_T36STG_20230218T210145.SAFE
- S2B_MSIL1C_20220817T084559_N0400_R107_T35SQB_20220817T093139.SAFE
- S2B_MSIL2A_20230809T083609_N0509_R064_T35SQB_20230915T115214

The data, available through the European Space Agency (ESA), was processed using the Sentinel Application Platform (SNAP) Desktop.

The selection of August as the focal month for this study stems from its representation of crucial climatic conditions in the region, particularly in the semi-arid context of Burdur Lake. This month aligns with the growing season, making it instrumental for understanding water dynamics, including the impact on vegetation and land-water interactions. Historical trends and local knowledge may underscore the significance of August, while the availability and reliability of Sentinel-2 imagery during this period contribute to more robust assessments. Opting for August across multiple years allows for direct and meaningful comparative analysis, aiding in the identification of recurring patterns or changes. Ultimately, the choice of August is intricately linked to the research objectives, ensuring that the selected timeframe aligns with the goals of studying drought conditions in Burdur Lake [11] .

The satellites carry a multispectral imager (MSI) that collects data in 13 bands with spatial resolutions ranging from 10 to 60 meters. The bands are used to monitor vegetation, water, and land use as shown in Table (1):

Table.1 Sentinel-2 Bands

Band	Wavelength (nm)	Resolution (m)	Applications
B1	443	60	Coastal aerosol
B2	490	10	Blue
B3	560	10	Green
B4	665	10	Red
B5	705	20	Red edge
B6	740	20	Near-infrared
B7	783	20	Near-infrared
B8	842	10	Near-infrared
B8A	865	20	Near-infrared
B9	940	60	Water absorption
B10	1375	60	Cirrus cloud detection
B11	1610	20	Short-wave infrared
B12	2190	20	Short-wave infrared

2.2 Spectral water index derivation

Multiple water indices were calculated using SNAP software, including Normalized Difference Water Index (NDWI), Modified NDWI (MNDWI), MNDWI5, and Automated Water Extraction Index (AWEI), to highlight water features. Thresholding techniques categorize pixels as either water or non-water based on the index values from these indices.

2.2.1 NDWI (Normalized Difference Water Index)

NDWI is a widely used spectral index in remote sensing and satellite imagery analysis. It serves as an effective tool for detecting the presence of water in various landscapes. The calculation of NDWI involves utilizing the near-infrared (NIR) and shortwave-infrared (SWIR) bands from satellite data. The formula for NDWI is straightforward as shown in Equation 1:

$$\mathrm{NDWI} = (NIR - SWIR) / (NIR + SWIR). \quad (1)$$

This index operates on a scale ranging from -1 to 1, with higher values indicating a higher likelihood of water presence. Generally, water bodies exhibit positive NDWI values, while land surfaces and other features display lower values. NDWI is instrumental in applications related to water resource management, hydrology, and land cover classification [6]. NDWI is widely used to identify surface water changes due to its sensitivity and easy interpretation but can also detect snow/ice and has noise contamination issues. In summary, while NDWI is simple and flexible, the other indices make trade-offs in noise reduction, vegetation suppression, and customization to different environments - improving water discrimination capability but requiring additional data and customization.

2.2.2 MNDWI (Modified Normalized Difference Water Index)

MNDWI is a specialized adaptation of the NDWI designed explicitly for water detection. It offers valuable

insights into the identification of water bodies within remote sensing imagery. MNDWI is computed using the green (G) and shortwave-infrared (SWIR) bands, and its formula shown in Equation 2:

$$MNDWI = (G - SWIR) / (G + SWIR). \quad (2)$$

Like NDWI, MNDWI values fall within the -1 to 1 range, with positive values signifying the presence of water. Researchers and professionals frequently utilize MNDWI in projects associated with wetland mapping, flood monitoring, and environmental assessments [7]. (MNDWI) enhances water discrimination from other land covers through the use of a SWIR band. However, it saturates over dense vegetation which reduces its utility in inundated forests.

2.2.3 *MNDWI5 (Modified Normalized Difference Water Index 5)*

MNDWI5 is an extension of the NDWI and MNDWI family of indices, serving a similar purpose of water body detection. It is constructed using the green (G) and shortwave-infrared (SWIR) bands. The MNDWI5 formula as shown in Equation 3:

$$MNDWI5 = (G - SWIR) / (G + SWIR + 0.5) \quad (3)$$

This index, much like its counterparts, delivers insights into the likelihood of water presence. Positive values in MNDWI5 are indicative of water, while negative values represent land or non-water features. Professionals and researchers employ MNDWI5 in applications such as lake monitoring, water quality assessments, and land cover analysis [12]. MNDWI5 implementation substitutes the SWIR band to mitigate dense vegetation saturation at the expense of some open water detection capacity.

2.2.4 *AWEI (Automated Water Extraction Index)*

AWEI is a versatile spectral index that plays a vital role in water feature detection and analysis. AWEI integrates information from multiple bands, typically including blue (B), green (G), and near-infrared (NIR). The specific formula shown in Equation 4:

$$AWEI = 4 \times (Green - 0.25 \times Red - 0.32 \times NIR - 0.25 \times SWIR2) \quad (4)$$

may vary depending on the intended application, but it generally combines these bands to identify water features. AWEI has proven effective in various areas, such as assessing water availability, mapping water bodies, and monitoring changes in aquatic ecosystems. Researchers and experts rely on AWEI to enhance their understanding of water-related phenomena and environmental dynamics [13]. AWEI) aims to tune water extraction algorithms to specific land cover types in a scene, enabling better early drought detection through characterization of variable terrain backgrounds. However, AWEI requires extensive calibration data and has a relatively complex formulation.

2.3 *Water mask generation*

Several studies have developed binary water masking approaches using thresholding of spectral water indices derived from satellite imagery. Common indices include the Normalized Difference Water Index (NDWI), Modified NDWI (MNDWI), MNDWI5, and Automated Water Extraction Index (AWEI) [6], [7], [13]. Thresholding techniques classify pixels as water or non-water based on index values. For example, McFeeters (1996) [6] originally proposed an NDWI threshold of zero for water body delineation.

In this study, we utilize a thresholding equation integrating four water indices.

While other studies have used thresholds on individual indices or dual index combinations, our equation incorporates four indices using OR logic for robust water extraction. The additional indices help better discriminate water under different environmental conditions. For instance, MNDWI5 enhances open water detection in urban areas. AWEI improves differentiation of water from dark surfaces like shade and shadow [13].

Compared to Li et al [14] who used NDWI and MNDWI, our equation adds MNDWI5 and AWEI, but does not incorporate MNDWI5. The unique combination of four indices in our methodology aims to optimize automated water mapping across diverse land cover types. We derive this multi-index thresholding equation based on published literature on the utility of different water indices for surface water extraction.

The study commenced with the importation of Sentinel-2 satellite imagery files into the Sentinel Application Platform (SNAP) desktop tool. The data underwent a resampling process within SNAP to homogenize spatial resolution, ensuring uniformity across all images for subsequent analyses. A focused examination on Burdur Lake was carried out through SNAP's subset operation (approximately 1068 km²), extracting the pertinent region of interest from the resampled Sentinel-2 data.

Spectral water indices, crucial for water body detection, were then computed from the subsetted Sentinel-2 data. These included the Normalized Difference Water Index (NDWI), Modified NDWI (MNDWI), and (AWEI). Subsequently, a binary water mask was generated using a thresholding technique. The thresholding logic, based on NDWI, MNDWI, MNDWI5, and AWEI, classified pixels as water (1) or non-water (0) as shown in Equation (5)

$$\begin{aligned} Water\ mask = {} & If\ (MNDWI \geq 0\ OR\ NDWI \\ & \geq 0\ OR\ MNDWI5 \\ & \leq 0\ OR\ AWEI \\ & \geq 0)\ Water\ mask \\ & = 1\ Else\ Water\ mask = 0 \end{aligned} \quad (5)$$

Note that: B means Band.

By combining multiple indices using an OR logic, a more inclusive water mask can be generated, with less omission of actual water pixels. Similar thresholding approaches have been widely used for water body extraction and flood mapping in various studies[15], [16], [17].

SNAP Desktop played a pivotal role in the entire methodology, overseeing resampling, subset extraction, spectral index computation, and water mask generation. This comprehensive approach ensured accuracy and reliability

throughout the process. The resulting TIFF images vividly depict the temporal changes in water extent in Burdur Lake over the study period.

Additionally, SNAP Desktop's significance extended to the preprocessing steps, ensuring data accuracy and reliability from subset extraction to the production of the water mask TIFF image. The use of SNAP's processing capabilities facilitated a consistent and standardized approach to image manipulation.

2.4 Clipping for accurate lake analysis

To ensure the precision and quality of the K-Means clustering results, a careful clipping process was implemented using QGIS. The water mask TIFF image, derived from the multi-temporal Sentinel-2 data, underwent a clipping operation. The objective was to isolate the water area specifically associated with Burdur Lake, mitigating the influence of surrounding features like farms and water infrastructure. Clipping was deemed essential to focus the analysis solely on the lake and enhance the accuracy of the K-Means clustering outcomes. This step guarantees that the subsequent assessments and quantifications accurately represent changes in the lake's water extent, providing a more reliable basis for drought monitoring.

2.5 K-Means clustering

K-means clustering is an uncomplicated unsupervised machine learning method for efficiently grouping unlabeled data by minimizing within-cluster variation through a repetitive procedure of cluster assignment and centroid recalculations [18].

The K-Means Clustering algorithm works by first arbitrarily choosing k starting points to represent initial cluster centers. It then groups each data point with the closest cluster center based on distance. After that, it recalculates the cluster centers by finding the mean of all data points assigned to that cluster. These steps of grouping points to their closest cluster and recalculating the cluster centers are repeated iteratively until the cluster assignments stop changing or a maximum number of iterations is met. The goal of K-Means is to minimize the total squared distance between data points and their cluster's centroid, as represented in the equation showing the sum of squared error criteria. In summary, K-Means iteratively groups data into k clusters by assigning points to their closest cluster center and recalculating the centers until an optimal configuration that minimizes the total within-cluster variance is reached. as shown in Equation (10):

$$\eta(m) = \Sigma(i=1 \text{ to } K)\ \Sigma(j=1 \text{ to } N)\ ||x(j) - c(i)||^2 \quad (10)$$

where:

K is the number of clusters, N is the number of data points

x(j) is the jth data point, c(i) is the centroid of the ith cluster,

||x(j) - c(i)||^2 is the squared Euclidean distance between the jth data point and the ith cluster centroid.

K-means clustering is one of the most commonly used unsupervised learning methods for classification tasks. Its straightforwardness, efficiency, and adaptability make K-means very appropriate for large-scale classification applications. K-means is uncomplicated to understand and put into practice. Compared to hierarchical clustering approaches, it has lower computational intricacy, allowing it to converge more rapidly when dealing with large data sets. The algorithm is also versatile - extensions like feature weighting and handling of non-spherical clusters have expanded its capabilities. One key advantage of K-means is that it inherently structures data by grouping similar points together. This data ordering can be helpful for additional analysis. The cluster centroids can be decoded as representative features that characterize each group. Visualizing and decoding K-means results is straightforward, providing insight into the data.

As K-means is capable of functioning in an unsupervised capacity, obviating the necessity for labelled training data, it results in the conservation of both financial resources and exertion otherwise expended in the acquisition of said data.

Points are assigned class labels based on their cluster memberships. The simplicity, speed, scalability, and unsupervised learning ability of K-means make it very well suited for classification problems, especially when dealing with large unlabelled datasets. K-means clustering has become a cornerstone unsupervised learning method for classification tasks.

The annual water masks were classified into water/non-water using K-means clustering. Water pixel percentages were calculated to assess changes over time using Python (see Appendix).

3 Results and discussions

3.1 Subset and resampled files

The Sentinel-2 satellite imagery underwent preprocessing steps in SNAP Desktop, including subset extraction and resampling. The resulting images provide a clear representation of the study area as seen in Figure 2.

3.2 Spectral water index derivation

Spectral water indices, such as NDWI, MNDWI, MNDWI5 and AEWI, were computed from the subsetted and resampled Sentinel-2 data. These indices play a crucial role in enhancing the detection of water bodies (colour bars added by Python) as seen in Figure 3 for 2019, Figure 4 for 2020, Figure 5 for 2021, Figure 6 for 2022 and Figure 7 for 2023.

3.3 Image processing for water detection refinement

A binary water mask was generated using a thresholding technique based on NDWI, MNDWI, MNDWI5, and AWEI. The resulting mask distinguishes water (1) and non-water (0) pixels.

To enhance water mask accuracy, the image underwent precise clipping and manual correction in QGIS, focusing on the study area boundaries. Subsequently, Python processing applied K-Means clustering to unveil temporal and spatial patterns in water bodies. This integrated approach ensures a comprehensive analysis of the study area's water dynamics, as seen in Figure 8.

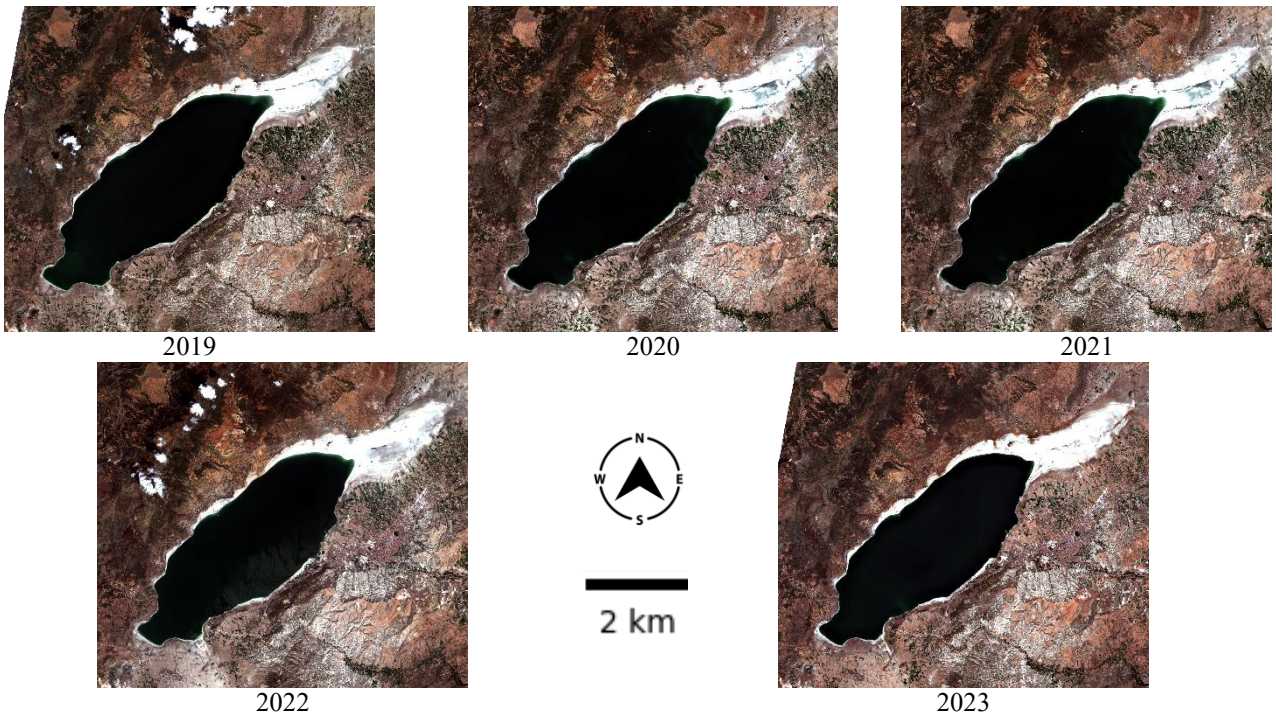

Figure. 2. Subset and resampled image

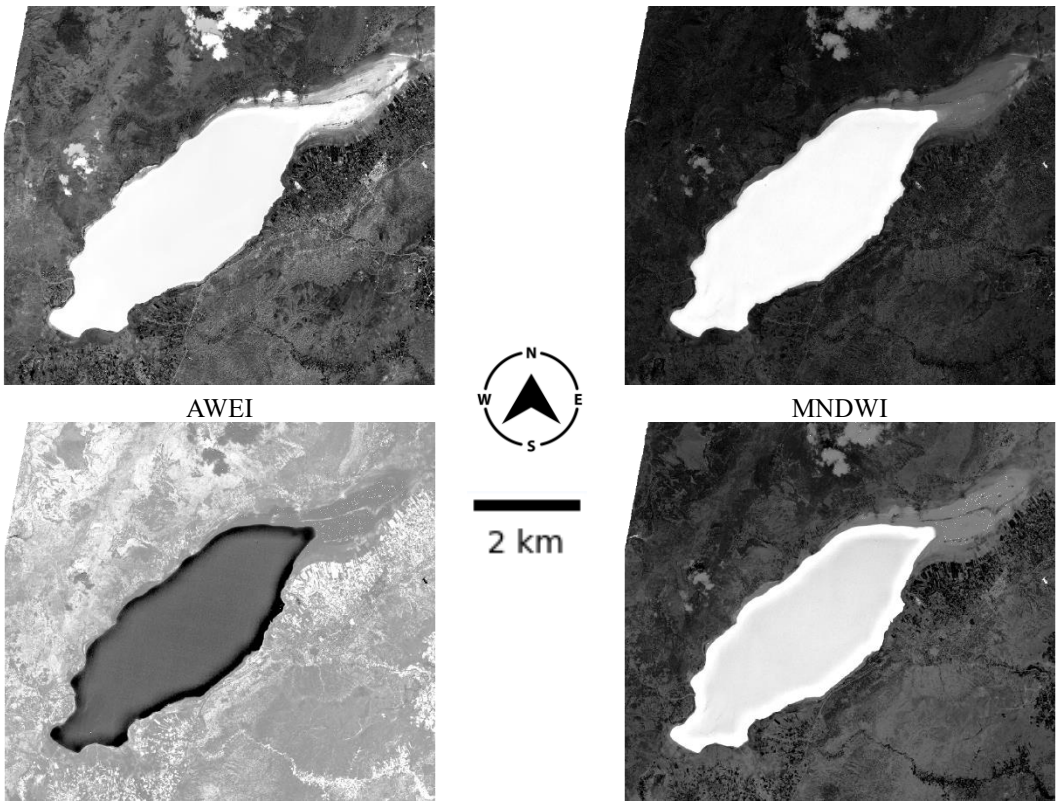

Figure. 3. Spectral water index derivation for 2019

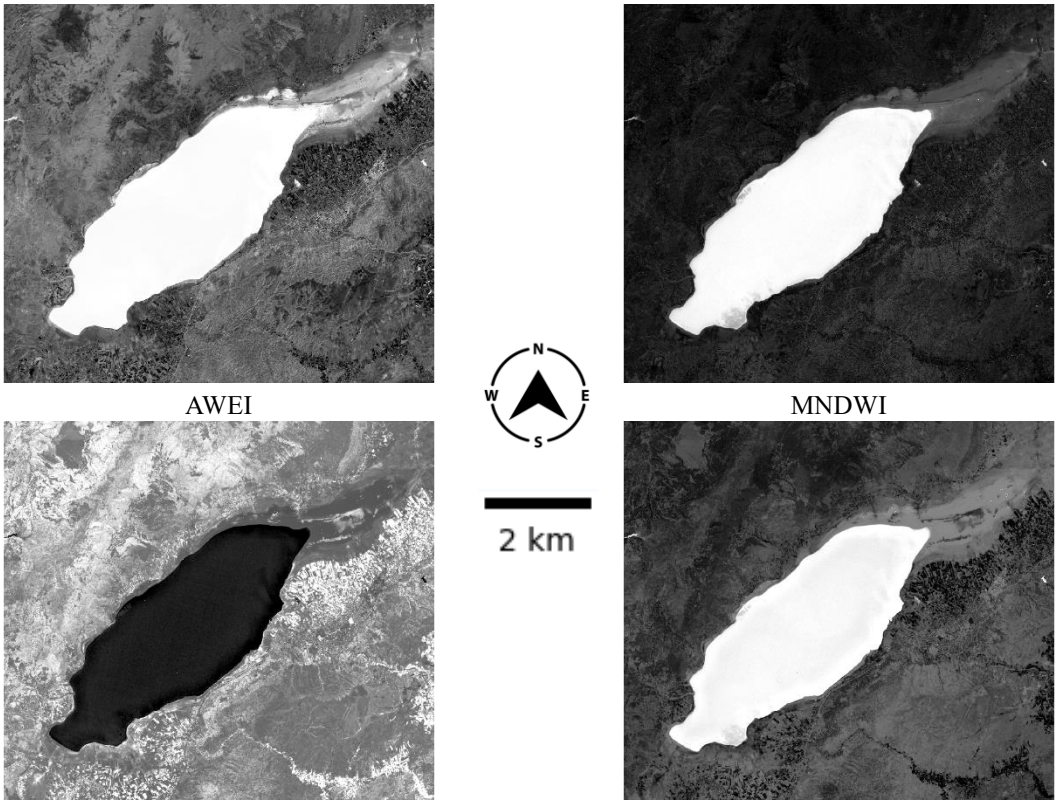

Figure. 4. Spectral water index derivation for 2020

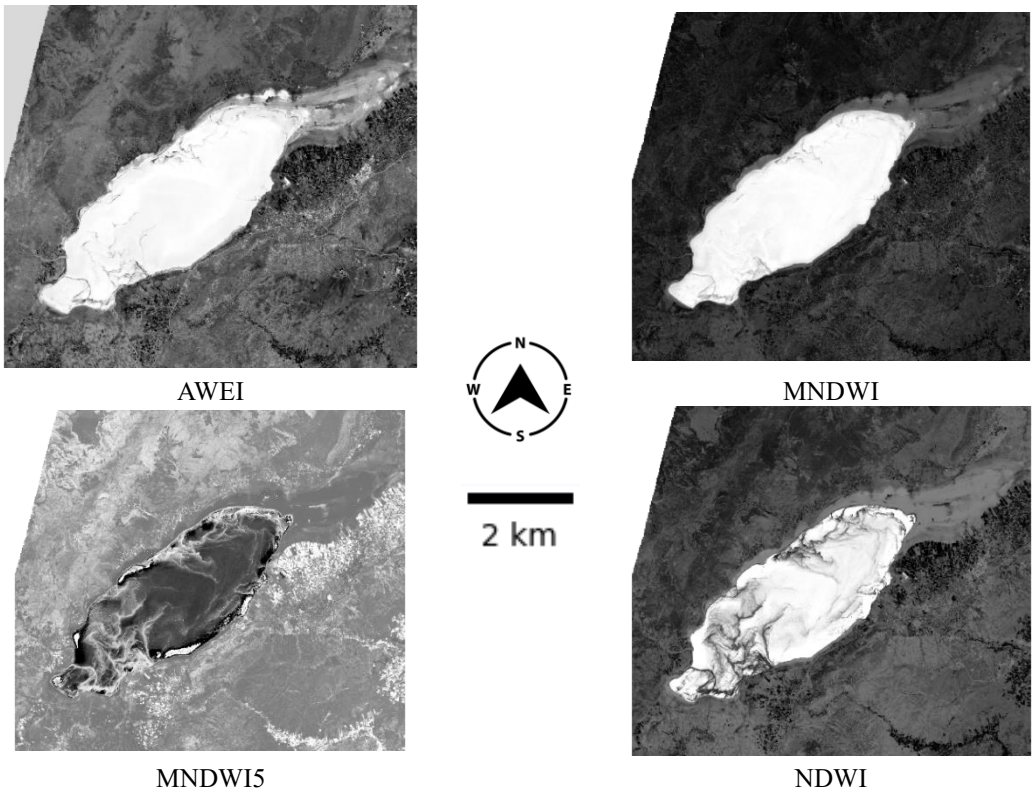

Figure. 5. Spectral water index derivation for 2021

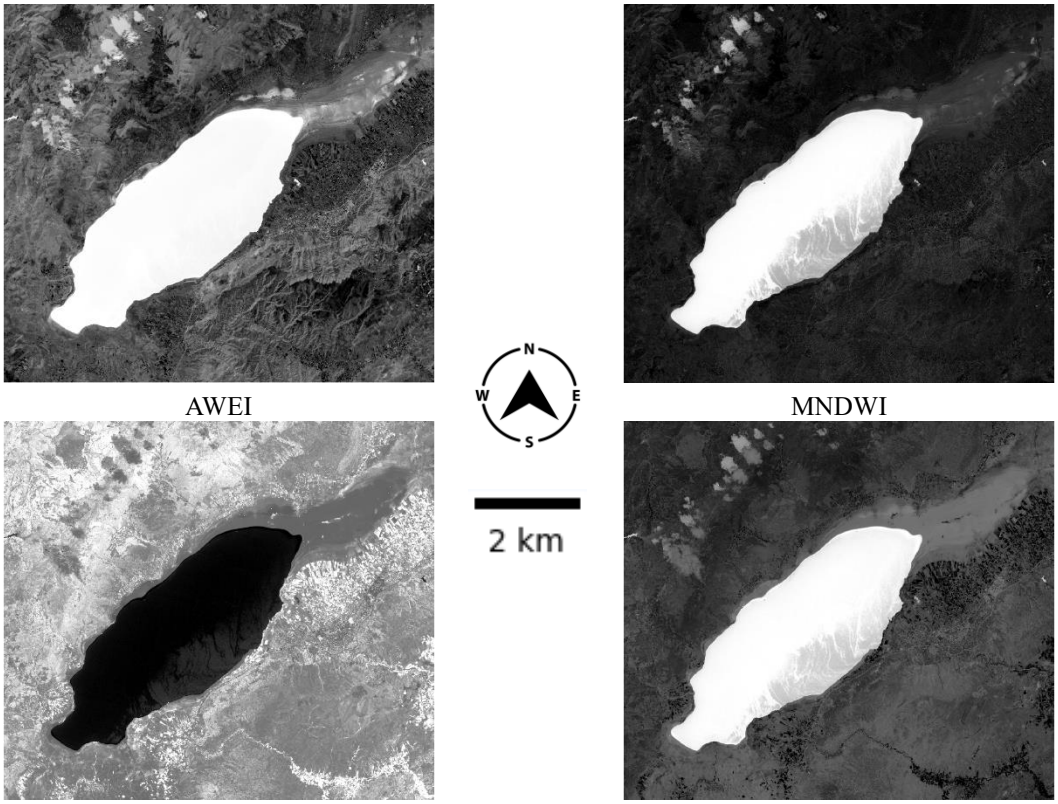

Figure. 6. Spectral water index derivation for 2022

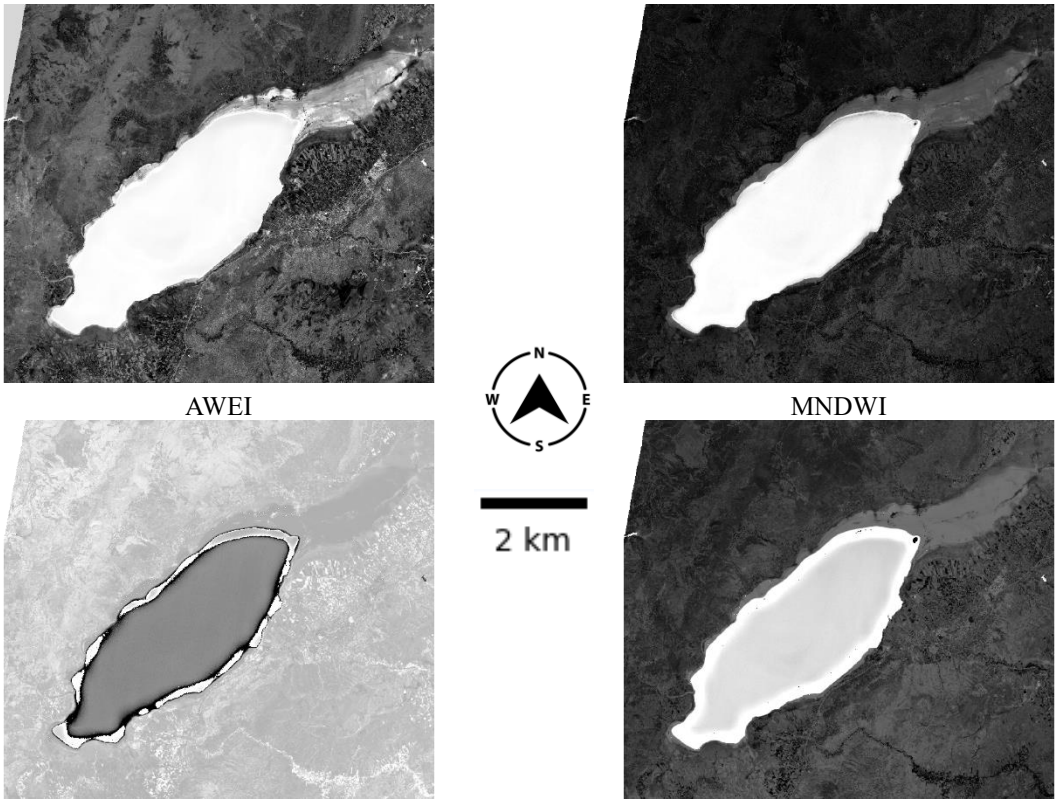

Figure. 7. Spectral water index derivation for 2023

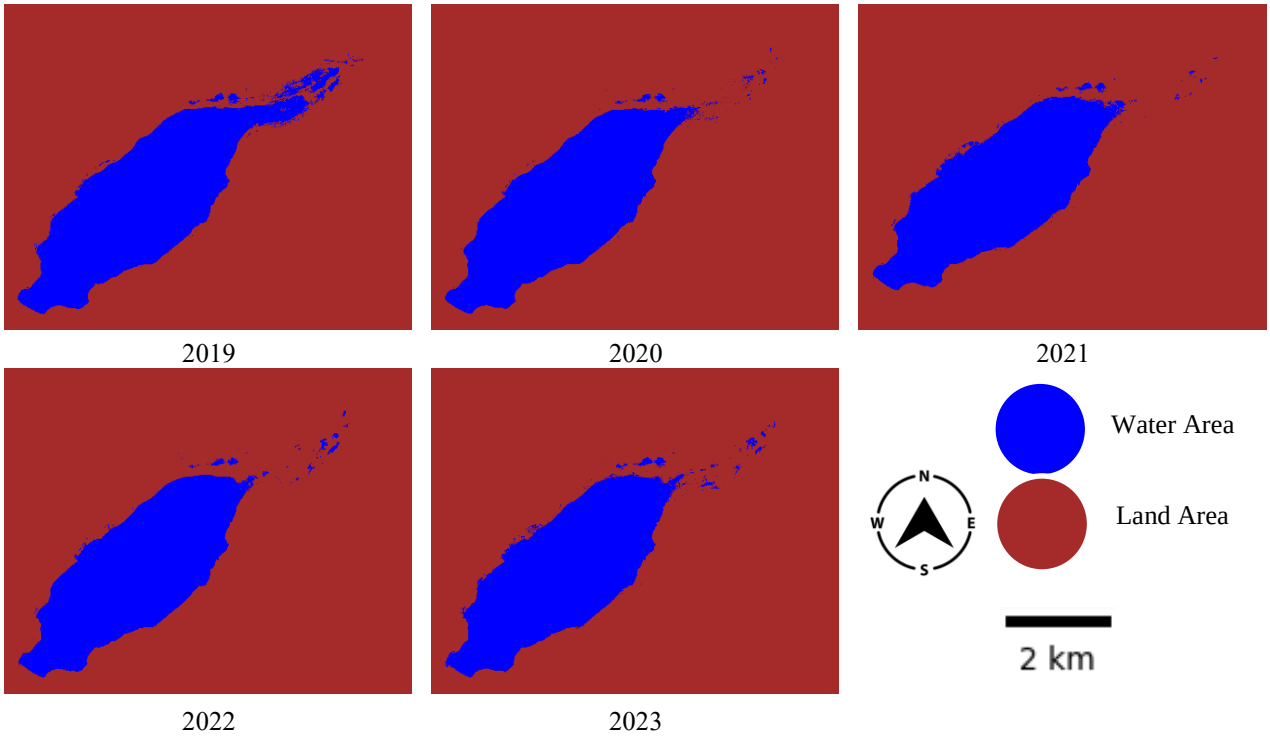

Figure. 8. Final result: water mask image

3.4 Time series analysis of lake water extent with clustering

Applying K-Means clustering on the water index images enabled effective quantification of the temporal variations in total water body coverage of Burdur Lake from 2019-2023 as shown in Table (2). The area values in the table were calculated by multiplying the percentage of water pixels by the total image area in square meters.

Table 2. Temporal Variation in Water Percentage (2019-2023)

No	Data	Area (km^2)	Water%	Change compared to 2019
1	2019	138.9456	18.53%	0%
2	2020	127.8732	17.06%	−7.96%
3	2021	125.9279	16.80%	−9.36%
4	2022	123.8665	16.52%	−10.86%
5	2023	124.7500	16.64%	−10.19%

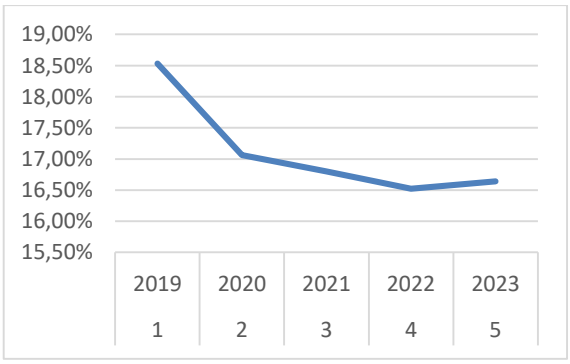

Figure 9. Time series of Burdur Lake's water coverage percentage from 2019-2023

The table presents the water percentage in Burdur Lake for each year from 2019 to 2023. The values indicate the proportion of water coverage in the lake for the respective years, highlighting any variations in water extent over the study period.

As the line chart trend in Figure 9 depicts, the lake exhibited a 10.3% reduction in the classified water extent area, decreasing from around 18.53% of total lake area in August 2019 to 16.64% by August 2023.

The chart's x-axis denotes the timespan in years, while the y-axis presents the mapped percentage of water pixels relative to the full lake area for each date. Visually, the line chart showcases the ability of the unsupervised clustering method to delineate the pronounced inter-annual fluctuations in Burdur's surface water coverage in response to drought. The captured trend highlights an overall drying period, with some volatility in specific years.

This demonstrates how K-Means clustering can produce insights into total water body spatial dynamics across time, quantifying expansion and contraction of lakes over multi-year climatic events. The revealed 10.3% ((18.53% - 16.64%) / 18.53% = 10.3%). decline in Burdur Lake's extent emphasizes concerning local impacts from regional drought conditions between 2019 and 2023.

The evaluation of Lake Burdur's water coverage alterations between 2019 and 2023, as presented in this study, offers fresh insights beyond the prior examination conducted by Sarp and Ozcelik [5] covering the period from 1987 to 2011. While both studies utilized satellite imagery to detect changes in surface area, this current research investigates a more recent timeframe employing distinct methodologies.

Unlike Sarp and Ozcelik, who utilized supervised SVM classification and spectral water indexes, this study introduces a novel approach employing unsupervised K-means clustering on water index images to delineate lake extents. The results reveal a continuous reduction in water coverage over the past five years, a trend not captured in the earlier study. Specifically, from 2019 to 2023, Lake Burdur experienced a notable 10.3% decrease in classified water area.

In comparison, Sarp and Ozcelik observed a 20% decline from 1987 to 2000 and a further 10% from 2000 to 2011. The higher temporal resolution in the current analysis provides fresh evidence of yearly fluctuations, underscoring the influence of drought conditions on the lake's size.

Overall, the utilization of unsupervised learning presents a novel technique for detecting changes in water bodies over time. The ongoing decline in Lake Burdur's water coverage highlighted in this study underscores the importance of frequent monitoring to track variations in response to climatic events. The contributions of this research include recent trends in water coverage and an enhanced methodology for assessing changes over multiple time periods.

4 Conclusions

This study presented a new methodology for quantifying drought impacts on lake water availability using multi-temporal Sentinel-2 analysis over Burdur Lake from 2019 to 2023. By combining widely used spectral water indices, binary masking techniques, and K-means classification, the approach effectively delineated and characterized a 10.3% decline in total lake water extent across the 5-year monitoring period.

The observed trend of decreasing water coverage signifies falling lake water availability, likely driven by shifting precipitation patterns and increasing evapotranspiration rates as regional warming accelerates. Operationally updated satellite measurements classified with machine learning algorithms can provide vital data to inform local water management policies amid more extreme, prolonged droughts.

As demonstrated in Burdur Lake, integrating Earth observations with water extraction methods can generate valuable time series analytics on inland water body variability in drylands worldwide. The framework's quantification of a full 10.3% reduction in lake area from 2019-2023 supports concerning conclusions of significant climate change impacts already materializing. More work must be done to monitor and conserve vulnerable water supplies as drought risk escalates.

In conclusion, the framework's analysis shows a reduction of 10.3% in lake area from 2019-2023, indicating significant impacts of climate change. This is consistent with previous studies by Sarp and Ozcelik, who observed a decline of 20% from 1987 to 2000 and a further 10% from 2000 to 2011. The current analysis provides new evidence of yearly fluctuations, highlighting the impact of drought conditions on the lake's size. These findings highlight the need for increased efforts to monitor and preserve at-risk water supplies as the risk of drought intensifies.

While powerful for retrospective analysis, pairing the demonstrated methodology with forecast data and consumption metrics could strengthen capabilities for predictive modelling scenarios to guide mitigation planning. This could aid stakeholders in protecting Burdur Lake as an essential ecosystem service under acute climate uncertainty moving forward over both near- and long-term horizons. The tools and Earth observation assets exist for science-based action.

Conflict of interest

The authors declare that there is no conflict of interest.

Similarity rate (iThenticate): 9%

References

[1] Y. O. Ouma and R. Tateishi, A water index for rapid mapping of shoreline changes of five East African Rift Valley lakes: an empirical analysis using Landsat TM and ETM+ data, Int J Remote Sens, vol. 27, no. 15, pp. 3153–3181, Aug. 2006, doi: 10.1080/01431160500309934.

[2] C. Giardino, M. Bresciani, P. Villa, and A. Martinelli, Application of Remote Sensing in Water Resource Management: The Case Study of Lake Trasimeno, Italy, Water Resources Management, vol. 24, no. 14, pp. 3885–3899, 2010, doi: 10.1007/s11269-010-9639-3.

[3] J. E. Pardo-Pascual, J. Almonacid-Caballer, L. A. Ruiz, and J. Palomar-Vázquez, Automatic extraction of shorelines from Landsat TM and ETM+ multi-temporal images with subpixel precision, Remote Sens Environ, vol. 123, pp. 1–11, Aug. 2012, doi: 10.1016/J.RSE.2012.02.024.

[4] J. H. Ryu, J. S. Won, and K. D. Min, Waterline extraction from Landsat TM data in a tidal flat: A case study in Gomso Bay, Korea, Remote Sens Environ, vol. 83, no. 3, pp. 442–456, Dec. 2002, doi: 10.1016/S0034-4257(02)00059-7.

[5] G. Sarp and M. Ozcelik, Water body extraction and change detection using time series: A case study of Lake Burdur, Turkey, Journal of Taibah University for Science, vol. 11, no. 3, pp. 381–391, 2017, doi: 10.1016/j.jtusci.2016.04.005.

[6] S. K. McFEETERS, The use of the Normalized Difference Water Index (NDWI) in the delineation of open water features, Int J Remote Sens, vol. 17, no. 7, pp. 1425–1432, May 1996, doi: 10.1080/01431169608948714.

[7] H. Xu, Modification of normalised difference water index (NDWI) to enhance open water features in remotely sensed imagery, Int J Remote Sens, vol. 27, no. 14, pp. 3025–3033, Jul. 2006, doi: 10.1080/01431160600589179.

[8] K. Rokni, A. Ahmad, A. Selamat, and S. Hazini, Water feature extraction and change detection using multitemporal landsat imagery, Remote Sens (Basel),

vol. 6, no. 5, pp. 4173–4189, 2014, doi: 10.3390/rs6054173.
[9] H. Gao, C. Birkett, and D. P. Lettenmaier, Global monitoring of large reservoir storage from satellite remote sensing, Water Resour Res, vol. 48, no. 9, 2012, doi: 10.1029/2012WR012063.
[10] W. Sun, B. Du, and S. Xiong, Quantifying sub-pixel surface water coverage in urban environments using low-albedo fraction from Landsat Imagery, Remote Sens (Basel), vol. 9, no. 5, May 2017, doi: 10.3390/rs9050428.
[11] E. Firatli, A. Dervisoglu, N. Yagmur, N. Musaoglu, and A. Tanik, Spatio-temporal assessment of natural lakes in Turkey, Earth Sci Inform, vol. 15, no. 2, pp. 951–964, Jun. 2022, doi: 10.1007/s12145-022-00778-8.
[12] R. R. Colditz, C. Troche Souza, B. Vazquez, A. J. Wickel, and R. Ressl, Analysis of optimal thresholds for identification of open water using MODIS-derived spectral indices for two coastal wetland systems in Mexico, International Journal of Applied Earth Observation and Geoinformation, vol. 70, pp. 13–24, Aug. 2018, doi: 10.1016/j.jag.2018.03.008.
[13] G. L. Feyisa, H. Meilby, R. Fensholt, and S. R. Proud, Automated Water Extraction Index: A new technique for surface water mapping using Landsat imagery, Remote Sens Environ, vol. 140, pp. 23–35, Jan. 2014, doi: 10.1016/j.rse.2013.08.029.
[14] W. Li et al., A comparison of land surface water mapping using the normalized difference water index from TM, ETM+ and ALI, Remote Sens (Basel), vol. 5, no. 11, pp. 5530–5549, 2013, doi: 10.3390/rs5115530.
[15] Y. Han et al., Water distribution based on SAR and optical data to improve hazard mapping, Environ Res, vol. 235, Oct. 2023, doi: 10.1016/j.envres.2023.116694.
[16] Y. Du, Y. Zhang, F. Ling, Q. Wang, W. Li, and X. Li, Water bodies' mapping from Sentinel-2 imagery with Modified Normalized Difference Water Index at 10-m spatial resolution produced by sharpening the swir band, Remote Sens (Basel), vol. 8, no. 4, 2016, doi: 10.3390/rs8040354.
[17] A. A. Davrawalska, Drought Monitoring with Sentinel-2 Case study: Western Cape Province, 2015-2020 training KIT-HYDR03, Nov. 2021. [Online]. Available: https://rus-copernicus.eu/portal/the-rus-library/learn-
[18] U. H. Atasever, A novel unsupervised change detection approach based on reconstruction independent component analysis and ABC-Kmeans clustering for environmental monitoring, Environ Monit Assess, vol. 191, no. 7, Jul. 2019, doi: 10.1007/s10661-019-7591-0.

Appendix

A. Software Tools and Data Source

This study exclusively utilized free-source software tools for data processing and analysis:

- Sentinel Application Platform (SNAP) Desktop: Employed for importing, preprocessing, and initial analysis of Sentinel-2 images.
- QGIS (Quantum Geographic Information System): Utilized for clipping the water mask image and manual removal of unwanted pixels.
- Visual Studio Code: Employed for coding and implementing the K-Means clustering algorithm.

B. Data Acquisition

- The Sentinel-2 satellite imagery for this study was obtained from the Copernicus Open Access Hub [^1^]. The images cover the period from 2019 to 2023 and were downloaded using the Copernicus Data Browser: https://dataspace.copernicus.eu/browser.

C. Code Implementation

- This study presents the implementation and analysis of K-Means clustering using (Python 3.12) by (Visual Studio Code 1.84.2) in (Windows 11 Home 23H2) as codded here: https://github.com/raqein/Drought-Monitoring-in-Burdur-Lake-Turkey-with-Water-Mask-using-K-Means-Clustering-.git.